



IVIVC Revised

Nikolaos Alimpertis^{1,2} · Antony Simitopoulos¹ · Athanasios A. Tsekouras^{3,2} · Panos Macheras^{1,2} 

Received: 16 October 2023 / Accepted: 29 December 2023 / Published online: 8 January 2024
© The Author(s), under exclusive licence to Springer Science+Business Media, LLC, part of Springer Nature 2024

Abstract

Purpose To revise the IVIVC considering the physiologically sound Finite Absorption Time (F.A.T.) and Finite Dissolution Time (F.D.T.) concepts.

Methods The estimates τ and τ_d for F.A.T. and F.D.T., respectively are constrained by the inequality $\tau_d \leq \tau$; their relative magnitude is dependent on drug's BCS classification. A modified Levy plot, which includes the time estimates for τ and τ_d was developed. IVIVC were also considered in the light of τ and τ_d estimates. The modified Levy plot of theophylline, a class I drug, coupled with the rapid (30 min) and very rapid (15 min) dissolution time limits showed that drug dissolution/absorption of Class I drugs takes place in less than an hour. We reanalyzed a carbamazepine (Tegretol) bioequivalence study using PBFTP models to reveal its complex absorption kinetics with two or three stages.

Results The modified Levy plot unveiled the short time span (~ 2 h) of the *in vitro* dissolution data in comparison with the duration of *in vivo* dissolution/absorption processes (~ 17 h). Similar results were observed with the modified IVIVC plots. Analysis of another set of carbamazepine data, using PBFTP models, confirmed a three stages absorption process. Analysis of steady-state (Tegretol) data from a paediatric study using PBFTP models, revealed a single input stage of duration 3.3 h. The corresponding modified Levy and IVIVC plots were found to be nonlinear.

Conclusions The consideration of Levy plots and IVIVC in the light of the F.A.T. and F.D.T. concepts allows a better physiological insight of the *in vitro* and *in vivo* drug dissolution/absorption processes.

Keywords carbamazepine · cyclosporine · finite absorption time · finite dissolution time · IVIVC · levy plot · oral drug absorption

Abbreviations

F.A.T.	Finite Absorption Time
F.D.T.	Finite Dissolution Time
IVIVC	<i>In vitro in vivo</i> correlations
PBPK	Physiologically Based Pharmacokinetic (PBPK) models
PBFTP	Physiologically Based Finite Time Pharmacokinetic (PBFTP) models

Introduction

The collapse of the physico-mathematical fallacy of infinite time of oral drug absorption [1–4], was followed by the development of the finite absorption time (F.A.T.) concept [5]. In this context, Physiologically Based Finite Time Pharmacokinetic (PBFTP) models, which rely on the principles: i) oral drug absorption processes take place in finite absorption time, τ and ii) zero-order drug input (single or multiple) because of the passive drug absorption under sink conditions, were developed [6]. The PBFTP models were applied successfully to a large number of experimental data and were found to be superior to the classical models based on the first-order absorption notion [3–7]. Meaningful parameters for drug's input rate(s) and duration of absorption stage(s) were estimated using nonlinear regression analysis.

A plausible, direct consequence of the F.A.T. concept is the consideration of the *in vivo* drug dissolution in terms of physiological time constraints. Intuitively, *in vivo* drug

✉ Panos Macheras
macheras@pharm.uoa.gr

¹ Faculty of Pharmacy, National and Kapodistrian University of Athens, Athens, Greece

² PharmaInformatics Unit, ATHENA Research Center, Athens, Greece

³ Department of Chemistry, National and Kapodistrian University of Athens, Athens, Greece

dissolution runs for a finite dissolution time (F.D.T), τ_d , which is equal to or shorter than F.A.T. In this vein, we recently introduced [8] the concept of Finite Dissolution Time (F.D.T.) as an intuitive extrapolation of (F.A.T.) concept [2]. This means that drug dissolution takes place under *in vivo* conditions for a finite time regardless of the complete or incomplete dissolution of the dose administered.

Official compendia USP [9] and the FDA guideline [10] define IVIVC as "the establishment of a relationship between a biological property, or a parameter derived from a biological property produced from a dosage form, and a physicochemical property of the same dosage form" and as "a predictive mathematical model describing the relationship between an *in-vitro* property of a dosage form and an *in-vivo* response". Since IVIVCs play a critical role in drug development and in optimization of formulations, numerous relevant publications can be found in the literature, e.g., PUBMED (9 October 2023) gives 20.005 results using the words "*in vitro in vivo* correlations drug". However, successful (Level A) [10] IVIVCs published in the literature are very limited despite the developments in our understanding of oral drugs absorption phenomena manifested by the regulatory adoption of biopharmaceutic classification system (BCS) and the biopharmaceutic drug disposition classification system (BDDCS) [11–15]. We quote the pessimistic assessment for IVIVC submissions with overall acceptance rate 40% of FDA scientists published in 2016: "... there is an imminent need for addressing the issues behind a low success rate in IVIVC development. The results from the current analysis revealed that special considerations should be taken in areas such as (a) selection of appropriate number/kind of formulations for IVIVC development/validation, (b) construction of exploratory plots to guide model building and selection, (c) investigation of the reasons of inconclusive predictability, (d) improvement on the quality and richness of the data, and (e) avoidance of over parameterization." [16].

We argue below that one of the major reasons of the low development of IVIVCs [16–18] is associated with the unphysical assumption of first-order oral drug absorption [1–4], which leads to the misconception of the exponential

nature of the % absorbed *versus* time plots [8]. In fact, the importance of the long overlooked F.A.T. concept in the correct construction of the percent absorbed *versus* time curves was just realized [8]. In this work, we consider the concepts of F.D.T. and F.A.T. in the realm of IVIVC.

Theory

It was recently shown [8] that the % absorbed *versus* time plots exhibit either a bilinear- or a multilinear-type shape when one single or more than one absorption stages are observed, respectively [6], Fig. 1.

In practice, the calculation of the % absorbed drug at various time points is based on modified Wagner-Nelson and Loo-Riegelman equations as described in [8]. This exercise obviously provides an upper limit for the *in vivo* drug dissolution process which operates for time τ_d , i.e., the finite dissolution time (F.D.T.), τ_d is necessarily less than τ ($\tau_d \leq \tau$). Usually, the times at which the same percentage is absorbed *in vivo* and dissolved *in vitro* are plotted in a Levy plot [19]. In this work, we propose a modified Levy plot, the so-called hereafter Levy-Macheras plot. Here, finite absorption time estimates τ (as described in [6, 8]) are displayed *versus in vivo* dissolution times τ_d set equal to τ . The time frame of the two processes, i.e., dissolution and absorption, are constrained by the inequality $\tau_d \leq \tau$, Fig. 2. This inequality relies on the fact that the duration of drug dissolution cannot be longer than the absorption process. In the extreme case that drug dissolution could happen beyond the absorption sites, namely, the termination of drug absorption, this will not affect the experimental pharmacokinetic data.

The classical IVIVC plots can be also considered in the light of τ_d and τ estimates. In a standard IVIVC plot % absorbed is plotted *versus* % dissolved *in vitro* for the same time duration. Under the F.A.T. premise the % absorbed drug changes linearly with time [8], hence one can map the % absorbed to a given fraction of τ . In the case of multiple absorption stages, the data analysis should be constrained up to the end of the first stage. So, in Fig. 3 we display %

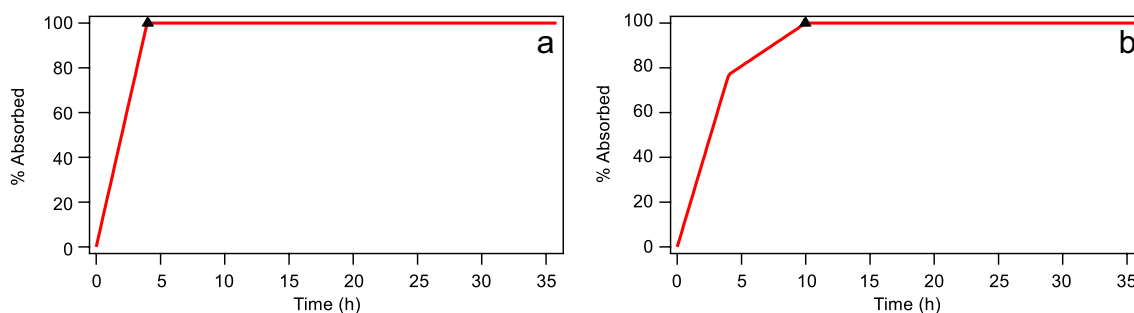


Fig. 1 Schematic of bilinear-type (a) or multilinear-type (b) % absorbed *versus* time plots calculated based on Eq. 2 of Ref. [8]. The intersection of the ascending last limb with the horizontal axis, denoted with a triangle, corresponds to the end of the absorption phase(s), τ [8].

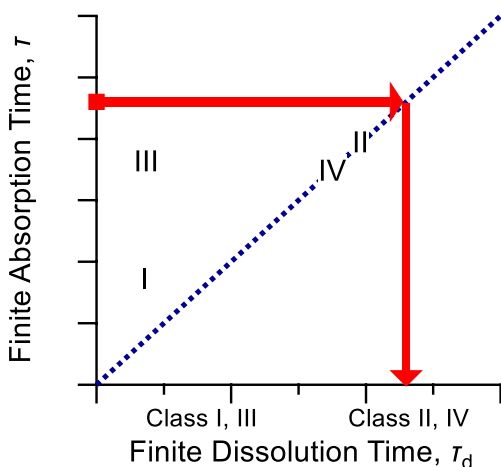


Fig. 2 The Levy-Macheras plot. The estimate for F.A.T., τ , defines the value of equal duration F.D.T., τ_d . In principle, for class I drugs $\tau_d \leq \tau$, for class III drugs $\tau_d < \tau$, while for class II and IV drugs $\tau_d = \tau$. The approximate positions of class I and III drugs is indicated by the respective symbols. The dotted line is the line of identity where class II and IV drugs are always located. The values of τ_d increase in the following order: (biowaivers), (Class I, III drugs), (Class II, IV drugs).

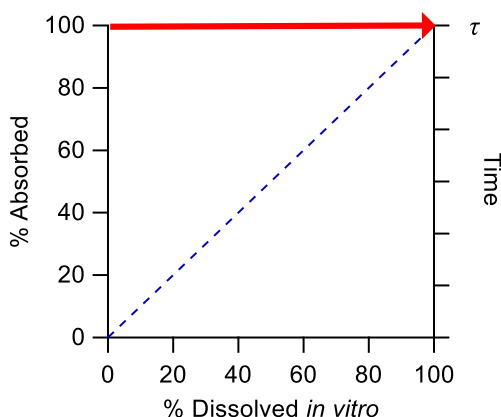


Fig. 3 Modified IVIVC plot. The right time axis, introduced here for the first time, corresponds to the *in vivo* data, because at time τ absorption is 100%. The dashed line is the identity line for a perfect IVIVC.

absorbed *versus* % dissolved *in vitro* and enhance the plot with an additional vertical time axis, which indicates the absorption progress with an upper limit the estimate for τ . On the new axis we can display critical time points such as the time for complete *in vitro* dissolution. Therefore, the *in vitro* and *in vivo* data, when plotted in the modified IVIVC (Fig. 3), can be easily contrasted with the value of τ , which is the upper limit for τ_d . This comparison provides a quick assessment of the relative magnitude of the *in vitro* dissolution process *versus* the actual percent absorbed drug at various time points under the prism of the estimate for τ ; this can be further used in the development of scaling factors between *in vitro* and *in vivo* data, if needed. Accordingly,

such plots provide not only the classical correlation information between the two variables plotted, but also the time evolution of the *in vitro* dissolution process in the realm of the boundary time limits τ and τ_d .

Results

The relative value of τ and τ_d for the various drug classes can be considered under the prism of Fig. 2. Also, modified IVIVC plots can be constructed using the drug examples examined below.

An estimate for τ of theophylline, which is a BCS Class I drug, derived from a bioequivalence study of immediate release formulations was found [20] equal to 0.75 (± 0.03) h. Since theophylline’s absorption is not dissolution limited, we present the two limits based on the dissolution criteria 15 and 30 min for very rapidly ($\geq 85\%$ dissolved in ≤ 15 min), and rapidly ($\geq 85\%$ dissolved in ≤ 30 min) dissolved drugs in the Levy-Macheras plot, (Fig. 4) along with the highest possible τ_d estimate for theophylline. We also plot in Fig. 4 the F.D.T. values obtained from visual inspection of the dissolution data of several drugs reported in the biowaiver monographs [21–35]. All these data demonstrate that both dissolution and absorption processes for BCS Class I drugs take place in less than an hour.

Carbamazepine is a Class II drug whose absorption has been studied extensively using dissolution, PBPK and bioequivalence studies, e.g., [37–40]. We first analyzed the concentration–time data of two carbamazepine bioequivalence studies using Tegretol as a reference product [37] based on percent absorbed *versus* time plots as described in [8] as well as nonlinear regression analysis using PBFTPK models [6]. In all cases the fittings using the PBFTPK models were superior to the classical models of first-order absorption. The best fitting results are presented in Figs. 5 and 6, while the estimates derived for the model parameters using the two methodologies are listed in Table I. These results show two input stages (B11 and B12 data sets) or three (B21 and B23 data sets) [37] with a decreasing as a function of time input rate. Remarkable similarity of the total duration, τ of carbamazepine absorption was found for all data derived from the two methodologies, Table I. The level of uncertainty for all estimates for τ was in the range 6% to 18% in terms of the corresponding coefficient of variation. The results listed in Table I unequivocally show that carbamazepine absorption takes place apart from small intestine in the colon too; since carbamazepine is a Class II drug, its dissolution continues in the colon up to time τ , namely, $\tau_d = \tau$ (Fig. 2), which is much longer than the mean intestinal transit time [5]. The heterogeneity prevailing in the colon in terms of hydrodynamic conditions, mobility, agitation, permeability results in a complex absorption profile (two or three absorption phases

Fig. 4 The Levy-Macheras plot for theophylline [20]. The F.D.T. values of various Class I drugs are also shown. The two time limits based on the dissolution criteria 15 and 30 min for very rapidly and rapidly dissolved drugs [36], respectively, are shown (vertical dashed lines).

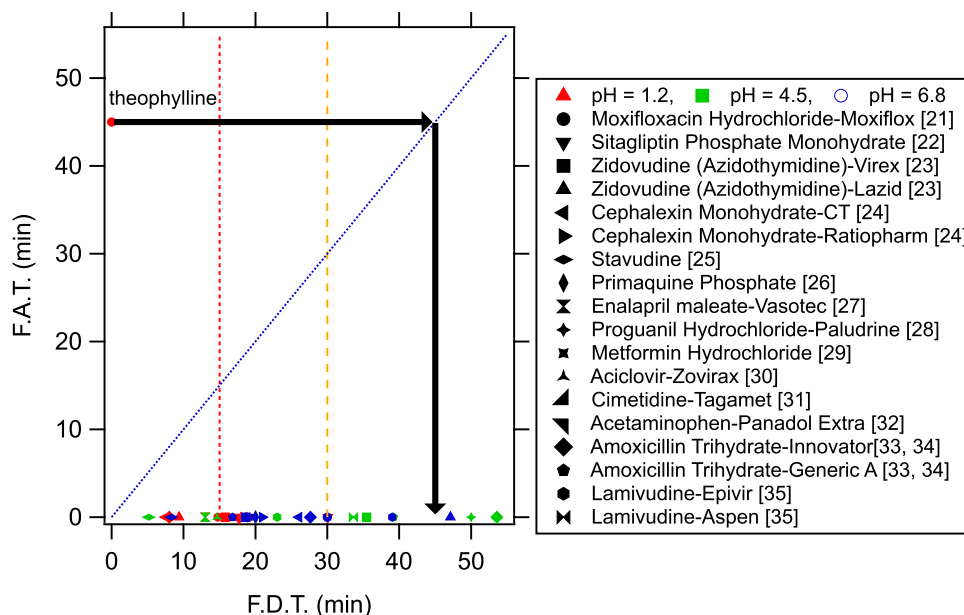
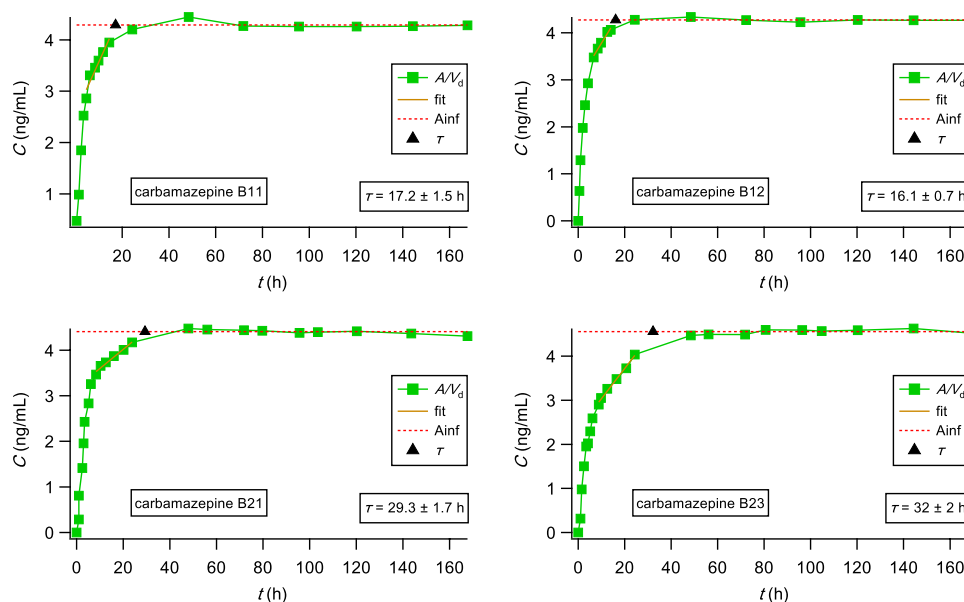


Fig. 5 Percent absorbed (expressed as apparent absorbed concentration [8]) versus time plot (green squares and solid line) for the carbamazepine formulations reported in [37]. The black triangle denotes the termination of drug absorption. The black dashed line is the simulation based on the model (Eq. 6 in [8]). The brown solid line is the fit of Eq. 6 to the last ascending segment data; the red dotted lines are the average level of the plateau values. Symbols have an identical meaning as defined in [8].



with a decreasing with time input rate of variable duration, Figs. 5 and 6), which is in full contrast with the smooth first-order absorption models applied routinely in pharmacokinetics using the Bateman function [1, 4]. All these “time dependent” absorption characteristics have been pointed out long time ago [41] and the term “heterogeneous drugs” like carbamazepine has been coined for Class II and IV drugs.

All these results allow us to re-plot the Levy plots reported in Ref. [37] as modified Levy-Macheras plots. Figure 7 is a representative example from a total of 8 reported in Fig. 3 of Ref. [37]; however, similar patterns were observed in all data analyzed. In line with Fig. 2, both axes in Fig. 7 have been expanded to 17 h, which corresponds to the total

duration of the carbamazepine *in vivo* dissolution/absorption. The equation provided in the original figure [37], corrected for the sign of the slope, gives an estimate for complete dissolution at 0.59 h. This result highlights the vast difference between the *in vitro* (0.59 h) and the *in vivo* (17 h) finite dissolution time.

In a similar vein, in Fig. 8 we show a modified IVIVC plot based on Fig. 4 of Ref. [37] in the form of Fig. 3. Obviously, we need to use time scaling to make the range of the *in vivo* and the *in vitro* times to be of the same order of magnitude and to lead to slopes around 1; the scaling factor used was 40. Thus, we generated Fig. 8 with the % absorbed *in vivo* as described in [8] and the original % dissolved *in vitro* from

Fig. 6 Best fit results of PBFTPK models [6] to carbamazepine blood concentration–time data reported in [37]. The symbol ▲ denotes the end of the absorption process. The top panel depicts the fit residuals. The formulations follow the code numbers reported in [37].

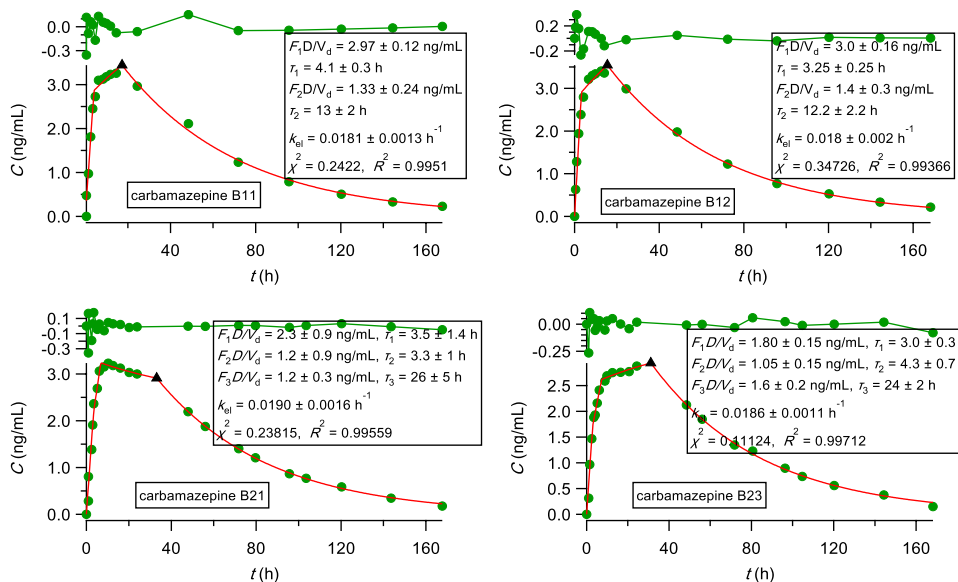


Table 1 Parameter Estimates for Carbamazepine Absorption Derived from % Absorbed vs Time Plots [8] and Nonlinear Regression Analysis using PBFTPK Models [6]

Data set [37]	τ from % absorbed vs time plots (hours)	s.d (hours)	τ from PBFTPK models (hours)	s.d.* (hours)
B11	17	2	17	2
B12	16	1	16	2
B21	29	2	33	5
B23	32	2	31	2

*based on fitting parameter errors and covariances

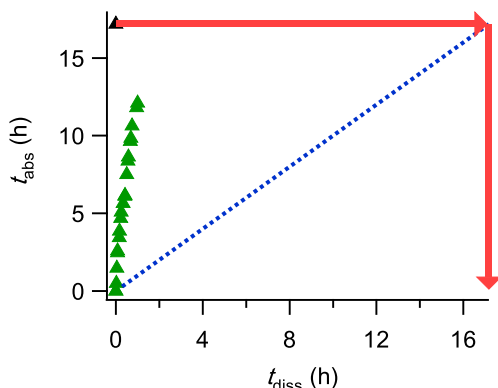


Fig. 7 Levy-Macheras plot for the carbamazepine data shown in the upper left panel of Fig. 3 reported in [37]. Both time axes have been extended to accommodate the long duration (τ) of carbamazepine absorption and the corresponding equal Finite Dissolution Time (τ_d).

[37]. Although the regression coefficient of the plot (Fig. 8) is 0.97, one notes the vast difference between the actual

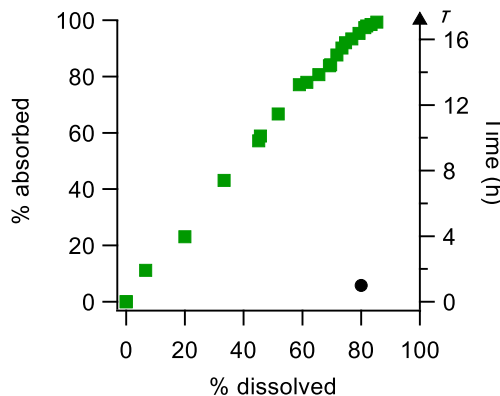


Fig. 8 % absorbed (B11) as analyzed in Fig. 5 and % dissolved (A11) for the reference formulation [37]. The IVIVC level A data shown in the upper left panel of Fig. 4 reported in [37] are re-plotted in the time frame of (τ , τ_d). The following parameters are shown on the time axis: the estimate for F.A.T. (τ) (triangle) and the time for maximum dissolution determined visually from the *in vitro* dissolution data (Fig. 2 of Ref. 37)) (circle).

completion of the absorption at 17 h and the achievement of 80% dissolution at 1 h.

We also analyzed using PBFTPK models the blood concentration–time data of the immediate release tablets of 400 mg carbamazepine data of the PBPB study [38]. Carbamazepine absorption follows complex kinetics with three successive input stages of total time of 33 (\pm 2) hours (see Fig. 9a). A very similar result was obtained by analyzing the % absorbed vs. time plot (see Fig. 9b) according to [8]. This analysis confirms the complexity of the carbamazepine absorption processes.

The last carbamazepine data we analyzed were derived from a 1991 relative bioavailability paediatric study with Tegretol as the reference formulation [39]. Here, we

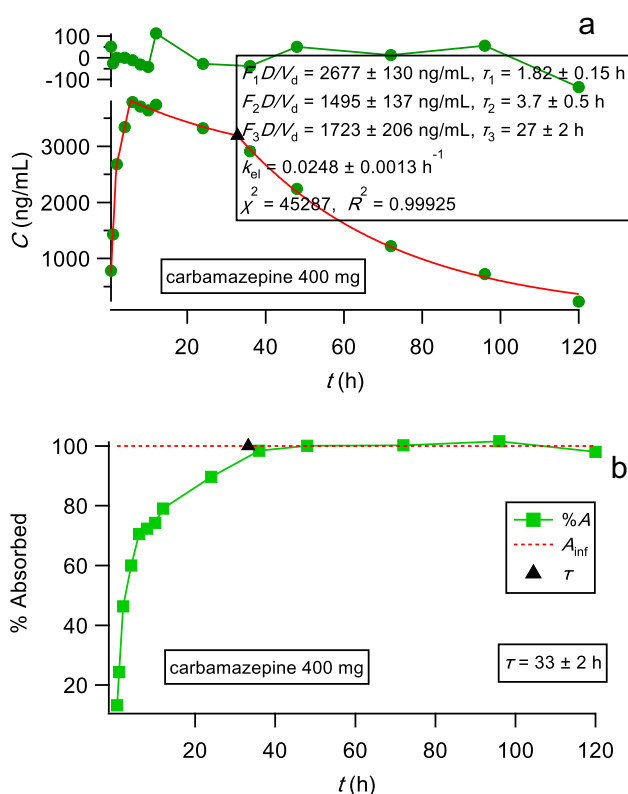


Fig. 9 Data [38] for orally administered 400 mg carbamazepine doses. **(a)** Fit to the data with zero-order absorption kinetics in three successive stages for a total of $33 (\pm 2)$ hours. **(b)** Analysis based on the % absorbed (green squares) on the same data shows absorption termination at $36 (\pm 2)$ hours (black triangle). Symbols as Figs. 5 and 6.

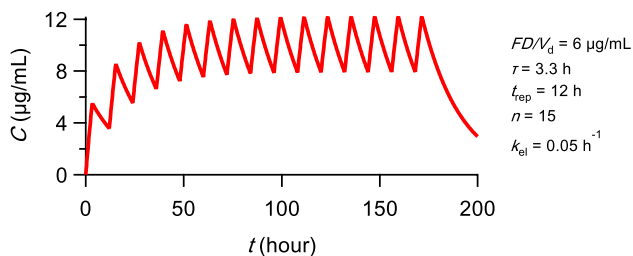


Fig. 10 Simulation of an abbreviated version of a repetitive carbamazepine administration scheme given in [39]. Zero-order absorption kinetics is assumed for 3.3 h postdose. n corresponds to the total number of doses administered; t_{rep} corresponds to the time interval between doses. The remaining parameters (FD/V_d , k_{el}) were chosen to make the simulation similar to the data analyzed.

estimated τ using a PBFTP model for multiple administration. A pool of children were administered twice daily a 200 mg dose for 6 weeks (i.e., 84 doses). The pharmacokinetic profile at steady-state was monitored after the last dose. Based on this scheme we performed a simulation assuming zero-order absorption kinetics and one-compartment disposition (see Appendix for the mathematical aspects of this approach). Using realistic parameter values (see Fig. 10) we

established that a steady-state pattern could be reached in less than a week. The data collected for the reference formulation in that study were thus shifted by 108 h.

Figure 11 shows the PBFTP analysis of the steady-state pharmacokinetic data of carbamazepine [39]. The data are described quite adequately by zero-order absorption kinetics in a one-compartment model (see Fig. 11a, b, c) with a total duration of absorption of 3.3 h. The complex and prolonged absorption of carbamazepine shown in Figs. 6 and 9 is not observed in Fig. 11. The reason is that carbamazepine C_{max} value ~ 10 $\mu\text{g/mL}$ at steady state is three times higher than the corresponding C_{max} values ~ 3 $\mu\text{g/mL}$ after single administration, Figs. 6 and 9. This implies a higher (about triple) carbamazepine elimination rate, which causes a much more rapid approach to a pseudo-steady state C_{max} overshadowing thus the complex carbamazepine absorption characteristics. This can also explain the higher elimination rate constant value found (0.056 h⁻¹) in the steady-state study than in the studies after single administration (0.018 h⁻¹, 0.025 h⁻¹), Figs. 6 and 9.

Figure 12b, derived from data [39] shown in Fig. 12a, shows that the Levy plot for the pediatric study is nonlinear. Similarly, the corresponding IVIVC plot exhibits nonlinearity, Fig. 12c. However, caution should be exercised in interpreting these results, Fig. 12b and c; since the drug elimination rate is higher at steady state, the absorption phase of carbamazepine has been “condensed” in terms of time.

Comparison of the 3 data sets analyzed shows a discrepancy in the order of magnitude of the drug concentrations in the blood. The first study indicates ng/mL concentrations, whereas the other two are in the $\mu\text{g/mL}$ range for administration of identical or comparable doses.

Discussion

This work is a plausible extension of the recently modified approach for the construction of the percent absorbed drug versus time plots using the F.A.T. concept [8]. Here, we reconsider Levy and IVIVC plots in the light of F.A.T. and F.D.T. concepts, which both constitute physiological time boundaries for the *in vivo* drug/dissolution absorption processes. The relative magnitude of the τ and τ_d estimates for F.A.T. and F.D.T., respectively are intuitively coupled with the four drug classes of the BCS, Fig. 2. For Class I and biowaiver drugs, the estimates for τ_d and τ can be further coupled with the regulatory dissolution limits for rapidly and very rapidly dissolved drugs [36] as shown in the Levy-Macheras plot, Fig. 4. For Class II drugs, the analysis of the *in vivo* carbamazepine data using the PBFTP models [6] and percent absorbed drug versus time profile [8], has a pivotal role for the estimation of the fundamental parameter, (F.A.T.), τ . In this context, the fitting results of PBFTP

Fig. 11 Steady-state drug concentrations after repetitive administration of carbamazepine. Data from [39]. (a) Fitting parameters are shown in the inset. It is assumed that the data were collected after the 10th dose (108 h and onwards), whereas in the study samples were collected after the 84.th dose, 996 h after the first dose. (b) In this fit, which is much better than the first one, the first and last drug concentration values have been replaced by their average. (c) Analysis [8] of % absorbed vs. time plot for the same data. Symbols as in Figs. 5 and 6.

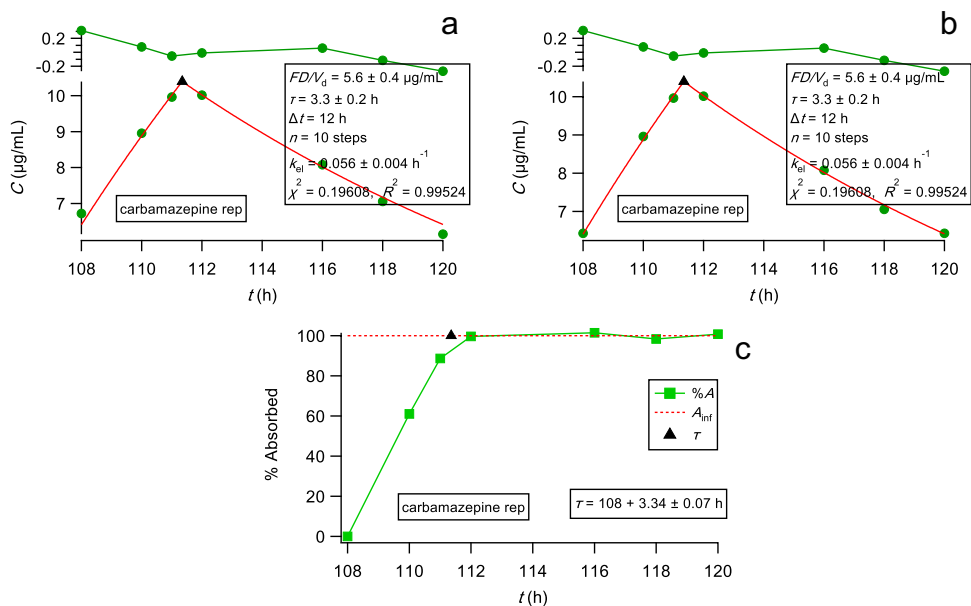
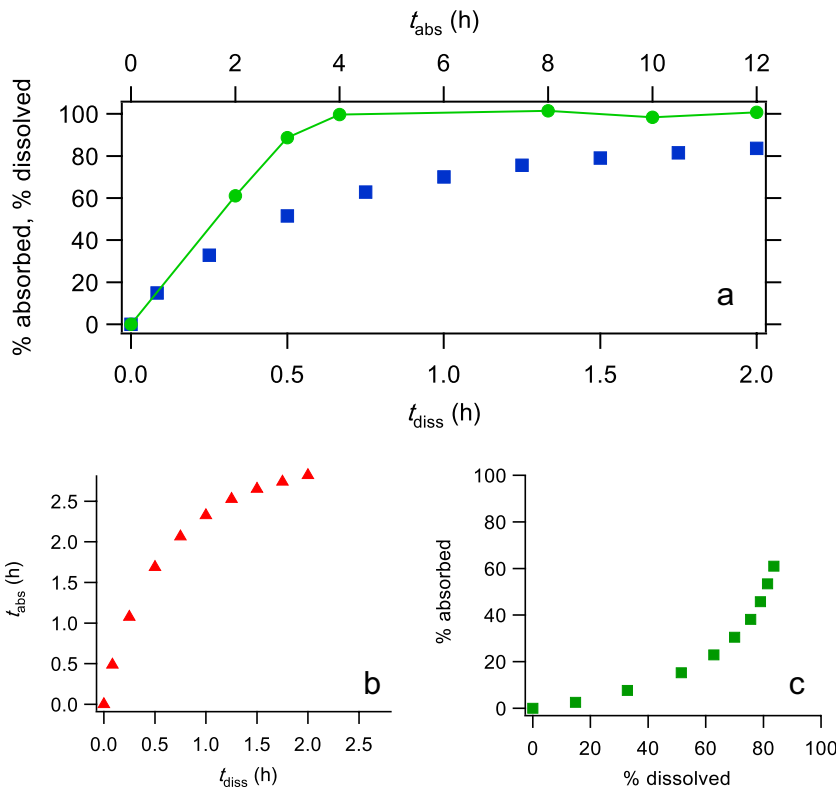


Fig. 12 (a) % absorbed (green circles) and % dissolved (blue squares) carbamazepine plotted together as a function of time reconstructed from the Tegretol data [39]. (b) Levy plot for the same data and (c) corresponding IVIVC plot.



models (Fig. 6, Table I) not only reveal the complex profile of carbamazepine absorption of the studied formulations [37], but also raise concerns with the traditional parameters C_{max} and t_{max} regarding their role in bioequivalence assessment. Thus, Fig. 6 shows that C_{max} is equal to C_{τ} for the data sets B₁₁, B₁₂ and B₂₃ while $C_{max} > C_{\tau}$ for the data set B₂₁; since C_{τ} corresponds to the end of the absorption and dissolution process, C_{max} also corresponds to the end of the

dissolution/absorption processes for the first three data sets. Besides, C_{max} is a pseudo steady-state parameter for the data set B₂₁ since $C_{max} > C_{\tau}$, Fig. 6. Consequently, C_{max} does not represent the classical rate parameter for all carbamazepine data sets examined and plotted in Fig. 6. These observations are in full agreement with the theoretical arguments concerning the role of C_{max} and C_{τ} pointed out in our previous studies [2, 4, 20].

It should be noted that the long duration, ~33 h, of carbamazepine absorption with three input stages was also observed, Fig. 9, in the analysis of the blood concentration–time data of the immediate release tablets of 400 mg carbamazepine data of the PBPK study [38]. One can see in Fig. 9 the gradually diminishing carbamazepine input rate as it moves down the gastrointestinal tract. However, this long diminishing with time absorption was not observed [6] with cyclosporine which is also a Class II drug. This means that the absorption characteristics of Class II drugs are not only drug related, but also formulation dependent; this is so since cyclosporine was administered as either a micro-emulsion or as a solution in olive oil [6]. A verification of the termination of cyclosporine absorption in the small intestine can also be based on the data [42] whereas an aqueous-ethanolic solution of cyclosporine was co-administered with milk, Fig. 13; this plot shows that cyclosporine absorption terminates at 1.86 ± 0.05 h, which implies cyclosporine absorption does not take place beyond the small intestines.

The modified Levy-Macheras plot (Fig. 7) of carbamazepine data provides a pictorial view not only for the correlation established in [37], but also the time evolution of the *in vitro* and *in vivo* data in relation to the physiologically sound τ and τ_d estimates for F.A.T. and F.D.T., respectively.

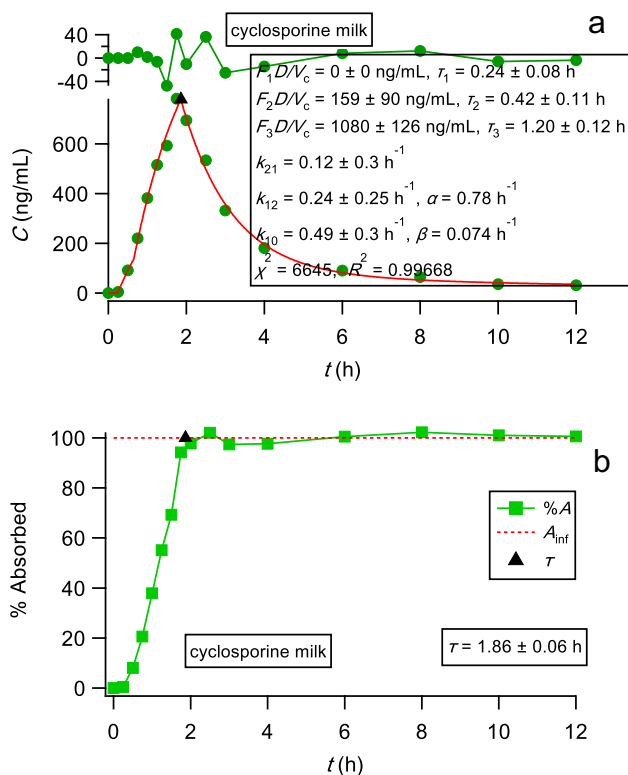


Fig. 13 (a) Best fitting results using PBFTP models [6] to cyclosporine data [42]. It is worth noticing that a lag time is obtained by assuming that the first input stage is of zero magnitude. (b) The corresponding percent absorbed vs. time plot [8]. Symbols as in Figs. 5 and 6.

Figure 7 shows that the time span of the correlated *in vitro* data is remarkably much shorter than 17 h, which is the estimated duration of dissolution/absorption processes under *in vivo* conditions, Table I. Therefore, it is advisable to utilize PBFTP models [6] or percent absorbed *versus* time plots [8] for the estimation of τ prior to the construction of the modified Levy-Macheras plot and IVIVC level A plots; obviously, this type of plot (Fig. 7) provides a physiologically sound boundary for the IVIVC data and helps the pharmaceutical scientist realize the time span of the IVIVC data in relation to F.A.T. and F.D.T. estimates. This is also clearly shown on the time axis of Fig. 8.

Figures 10–12 deliver a very important message concerning the bioequivalence studies for highly variable drugs. For the first time the diminution of the duration of absorption at steady state is quantified explicitly, namely, ~5 times (17 h / 3.3 h) for the example examined. Thus, the results presented in Fig. 11b and c should be considered with caution since they do not represent the real picture of a Levy or IVIVC plot after a single carbamazepine dose administration. However, the reduction of the absorption phase variability for the highly variable drugs/formulations is explicitly shown here, Fig. 11 *versus* Figs. 5, 6 and 9; this justifies the execution of bioequivalence studies under steady-state conditions [43].

Besides, the results of this study in conjunction with results of the previous studies [5, 6, 8] have a tremendous impact in the following two topics of extreme importance for the pharmaceutical scientist in academia, industry, and regulatory Agencies.

Drug Dissolution Impact The dream for an *in vitro* dissolution test predictable of *in vivo* behaviour was started almost forty years ago. For example, milk was proposed as the first dissolution biomedium to mimic fed conditions in 1986 [44, 45]. In the late 1990s this first approach was the starting point for the development of incalculable biorelevant media with a very limited success in terms of the IVIVC developed and their predictability [13, 16]. All these studies focused exclusively on the composition of the dissolution medium, while important aspects of drug dissolution associated with the recently developed F.A.T. and F.D.T. concepts have been overlooked, namely, drug dissolution/absorption take place in a finite time and operate under sink conditions [4, 5]; a linear increase over time of the % absorbed drug was recently found [8] and short, e.g., cyclosporine [6], Fig. 13 or long, e.g., carbamazepine (Figs. 5, 6, Table I) duration of absorption, which are both Class II drugs, were observed. These features can be considered in the design of a predictable dissolution test by developing a biphasic one vessel system [46, 47] which is most akin to the *in vivo* conditions maintaining sink conditions and allow linear increase of the dissolved drug amount in the organic layer facilitating thus IVIVC. Besides, reduction of dissolution and input rates can

be accommodated with a proper change of the surface area between the aqueous and organic layers in accord with the anatomic/physiological diminution of the surface area of the gastrointestinal membrane in the colon in comparison with the small intestines [38]. In addition, published studies [40] on the importance of the volume of the dissolution medium for adults and paediatric patients and its agitation can be considered too. Work is in progress for the development of such a dissolution system.

Development of Generics The analytical power of PBFTP models [6] coupled with the modified percent absorbed *versus* time plots developed in [8] can provide estimates for τ by analyzing the *in vivo* data of the reference (innovator's) product published in the literature. The fitting results of PBFTP models can be easily coupled with the *in vitro* dissolution data of the reference formulation in all compendia media to develop the Levy-Macheras plot and IVIVC level A, if any, or IVIV relationships. All these results for the reference formulation formulate a “map” which can be used as a guide for the development of the generic formulation. For example, if a strong IVIVC level A for the reference formulations has been established, this finding necessitates a very strong correlation between the *in vitro* data of the reference and test (generic) formulation, e.g., high F_2 values. On the contrary, a weak relationship between the *in vitro* and *in vivo* data of the reference formulation rules out the importance of the dissolution tests and points to other factors, which are important for the *in vivo* drug absorption, e.g., permeability or stability issues.

Needless to say that the above exercise can be carried out using reference formulations for a large number of drugs. The fitting results using PBFTP models [6] and modified % absorbed *versus* time plots [8] as well as the Levy-Macheras plot and the IVIVC correlations will be of high interest for the pharmaceutical scientist since structure based-dissolution/absorption relationships can be developed.

Finally, interested readers can contact the authors for the use of PBFTP software, which is not commercially available as yet.

Conclusions

The development of F.A.T. and F.D.T. concepts offers a new consideration of the oral drug absorption phenomena. The relative magnitude of τ and τ_d estimates is related to BCS class of the drug considered, Fig. 2; these estimates are used for the construction of novel Levy-Macheras plots, which allow the comparison of the time evolution of the *in vitro* dissolution data with the actual observed in practice termination of

the drug absorption stage(s). The modified IVIVC plots, apart from the statistical correlation developed, depict the time span of the *in vitro* and the *in vivo* data and help the pharmaceutical scientist realize their utility and validity in terms of drug's absorption predictability. We envisage dissolution research towards the development of two layers one vessel systems most akin to the *in vivo* conditions relying on all physiologically related concepts delineated above. These *in vitro* results, if analyzed with the Levy-Macheras plot and the modified IVIVC plots developed herein, can lead to more, better, and predictive IVIVC altering the prevailing pessimistic view [16].

Appendix

We list below the analytical expressions for 4 cases of drug concentration in the blood as a function of time after oral administration for the one-compartment model with zero-order, finite time absorption kinetics in one or more stages.

1 Single input stage of duration τ .

For $0 < t \leq \tau$,

$$C(t) = \frac{FD}{\tau V_d k_{el}} (1 - e^{-k_{el}t}) \quad (1)$$

$$C(\tau) = \frac{FD}{\tau V_d k_{el}} (1 - e^{-k_{el}\tau}) \quad (2)$$

For $\tau < t$,

$$C(t) = C(\tau)e^{-k_{el}(t-\tau)} \quad (3)$$

2 Two consecutive input stages of duration τ_1 and τ_2 .

For $0 < t \leq \tau_1$,

$$C(t) = \frac{F_1 D}{\tau_1 V_d k_{el}} (1 - e^{-k_{el}t}) \quad (4)$$

$$C(\tau_1) = \frac{F_1 D}{\tau_1 V_d k_{el}} (1 - e^{-k_{el}\tau_1}) \quad (5)$$

For $\tau_1 < t \leq \tau_1 + \tau_2$,

$$C(t) = C(\tau_1)e^{-k_{el}(t-\tau_1)} + \frac{F_2 D}{\tau_2 V_d k_{el}} (1 - e^{-k_{el}(t-\tau_1)}) \quad (6)$$

For $\tau_1 + \tau_2 < t$,

$$C(t) = C(\tau_1 + \tau_2)e^{-k_{el}(t-\tau_1-\tau_2)} \quad (7)$$

3 n consecutive input stages each of duration τ_i .

For $0 < t \leq \tau_1$,

$$C(t) = \frac{F_1 D}{\tau_1 V_d k_{el}} (1 - e^{-k_{el} t}) \quad (8)$$

For $\sum_{j=1}^{i-1} \tau_j < t \leq \sum_{j=1}^i \tau_j$,

$$C(t) = C\left(\sum_{j=1}^{i-1} \tau_j\right) e^{-k_{el}(t - \sum_{j=1}^{i-1} \tau_j)} + \frac{F_i D}{\tau_i V_d k_{el}} \left(1 - e^{-k_{el}(t - \sum_{j=1}^{i-1} \tau_j)}\right) \quad (9)$$

For $\sum_{j=1}^n \tau_j < t$,

$$C(t) = C\left(\sum_{j=1}^n \tau_j\right) e^{-k_{el}(t - \sum_{j=1}^n \tau_j)} \quad (10)$$

4 One input stage of duration τ coupled with n identical doses administered at equal Δt intervals.

For $i\Delta t < t \leq \tau + i\Delta t$, where i is an integer with $0 \leq i < n$

$$C(t) = C(i\Delta t) e^{-k_{el}(t - i\Delta t)} + \frac{FD}{\tau V_d k_{el}} (1 - e^{-k_{el}(t - i\Delta t)}) \quad (11)$$

where $C(0) = 0$

For $\tau + i\Delta t < t \leq (i + 1)\Delta t$ or $\tau + n\Delta t < t$,

$$C(t) = C(\tau + i\Delta t) e^{-k_{el}(t - (\tau + i\Delta t))} \quad (12)$$

The latter set of equations was used to generate Fig. 10 and analyze the data shown in Fig. 11.

Acknowledgements This work is dedicated to all students who maintain respect to their teachers.

Funding This work received no funding.

Declarations

Conflict of Interest The authors declare no conflict of interest.

References

- Macheras P. On an unphysical hypothesis of Bateman equation and its implications for pharmacokinetics. *Pharm Res.* 2019;36:94. <https://doi.org/10.1007/s11095-019-2633-4>.
- Tsekouras AA, Macheras P. Columbus' egg: Oral drugs are absorbed in finite time. *Eur J Pharm Sci.* 2022;176:106265. <https://doi.org/10.1016/j.ejps.2022.106265>.
- Macheras P, Tsekouras AA. The Finite Absorption Time (FAT) concept en route to PBPK modeling and pharmacometrics. *J Pharmacokinet Pharmacodyn.* 2023;50:5–10. <https://doi.org/10.1007/s10928-022-09832-w>.
- Macheras P, Tsekouras AA. Revising Oral Pharmacokinetics, Bioavailability and Bioequivalence Based on the Finite Absorption Time Concept. Cham: Springer; 2023. <https://doi.org/10.1007/978-3-031-20025-0>.
- Macheras P, Chryssafidis P. Revising pharmacokinetics of oral drug absorption: I models based on biopharmaceutical/physiological and finite absorption time concepts. *Pharm Res.* 2020;37:187. <https://doi.org/10.1007/s11095-020-02894-w>. Erratum. *Pharm Res* 2020;37:206. <https://doi.org/10.1007/s11095-020-02935-4>.
- Chryssafidis P, Tsekouras AA, Macheras P. Re-writing oral pharmacokinetics using physiologically based finite time pharmacokinetic (PBFTPK) models. *Pharm Res.* 2022;39:691–701. <https://doi.org/10.1007/s11095-022-03230-0>.
- Wu D, Tsekouras AA, Macheras P, Kesiosoglou F. Physiologically based pharmacokinetic models under the prism of the finite absorption time concept. *Pharm Res.* 2023;40:419–29. <https://doi.org/10.1007/s11095-022-03357-0>.
- Alimpertis N, Tsekouras AA, Macheras P. Revamping Biopharmaceutics-Pharmacokinetics with Scientific and Regulatory Implications for Oral Drug Absorption. *Pharm Res.* 2023;40:2167–75. <https://doi.org/10.1007/s11095-023-03578-x>.
- United States Pharmacopeia (2022). General Chapter, (1088) in Vitro and in Vivo Evaluation of Oral Dosage Forms. USP-NF. Rockville, MD: United States Pharmacopeia. https://doi.org/10.31003/USPNF_M99807_04_0.
- FDA Guidance for Industry Extended Release Oral Dosage Forms: Development, Evaluation, and Application of In Vitro/In Vivo Correlations. Office of Training and Communications Division of Communications Management. The Drug Information Branch, HFD-210 5600 Fishers Lane Rockville, MD 20857.
- Amidon GL, Lennernäs H, Shah VP, Crison JR. A theoretical basis for a biopharmaceutic drug classification: the correlation of in vitro drug product dissolution and in vivo bioavailability. *Pharm Res.* 1995;12:413–20. <https://doi.org/10.1023/a:1016212804288>.
- Wu C, Benet L. Predicting drug disposition via application of BCS: transport/absorption/ elimination interplay and development of a biopharmaceutics drug disposition classification system. *Pharm Res.* 2005;22:11–23. <https://doi.org/10.1007/s11095-004-9004-4>.
- Charalabidis A, Sfouni M, Bergström C, Macheras P. The Biopharmaceutics Classification System (BCS) and the Biopharmaceutics Drug Disposition Classification System (BDDCS): Beyond guidelines. *Int J Pharm.* 2019;566:264–81. <https://doi.org/10.1016/j.ijpharm.2019.05.041>.
- Food and Drug Administration. Center for Drug Evaluation and Research (CDER). Waiver of In Vivo Bioavailability and Bioequivalence Studies for Immediate-Release Solid Oral Dosage Forms Based on a Biopharmaceutics Classification System. Guidance for Industry U.S. Department of Health and Human Services. 2017. <http://resource.nlm.nih.gov/101720038>
- European Medicines Agency. Committee for medicinal products for human use (CHMP) Guideline on the investigation of bioequivalence. London, Jan. 2010. https://www.ema.europa.eu/en/documents/scientific-guideline/guideline-investigation-bioequivalence-rev1_en.pdf
- Suarez-Sharp S, Li M, Duan J, Shah H, Seo P. Regulatory Experience with In Vivo In Vitro Correlations (IVIVC) in New Drug Applications. *AAPS J.* 2016;18(6):1379–90. <https://doi.org/10.1208/s12248-016-9966-2>.
- Mircioiu C, Mircioiu I, Voicu V, Miron D. Dissolution–bioequivalence non-correlations. *Basic Clin Pharmacol Toxicol.*

- 2005;96:262–4. <https://doi.org/10.1111/j.1742-7843.2005.pto960324.x>.
18. Dokoumetzidis A, Macheras P. IVIVC of controlled release formulations: Physiological-dynamical reasons for their failure. *J Control Release*. 2008;129:76–8. <https://doi.org/10.1016/j.jconrel.2008.04.005>.
 19. Certrara, Levy-Plots, <https://onlinehelp.certara.com/phoenix/8.3/topics/levyplots.htm>. Accessed 4 Jan 2024
 20. Chryssafdis P, Tsekouras AA, Macheras P. Revising pharmacokinetics of oral drug absorption: II bioavailability bioequivalence considerations. *Pharm Res*. 2021;38:1345–56. <https://doi.org/10.1007/s11095-021-03078-w>.
 21. Saelim N, Suksawaeng K, Chupan J, Techatanawat I. Biopharmaceutics classification system (BCS)-based biowaiver for immediate release solid oral dosage forms of moxifloxacin hydrochloride (Moxiflox GPO) manufactured by the Government Pharmaceutical Organization (GPO). *Asian J Pharmaceut Sci*. 2016;11:235–6. <https://doi.org/10.1016/j.ajps.2015.11.016>.
 22. Lange ADC, Batistel AP, Sfair LL, Carlosso J, Volpato NM, Schapoval ESS. Sitagliptin Phosphate: Development of a Dissolution Method for Coated Tablets Based on In Vivo Data for Improving Medium Sensitivity. *Dissolution Technol*. 2014;2014(5):17–22. <https://doi.org/10.14227/DT210214P17>.
 23. Ocheke NA, Ngwuluka NC, Owolayo H, Fashedemi T. Dissolution Profiles of Three Brands of Lamivudine and Zidovudine Combinations in the Nigerian Market. *Dissolution Technol*. 2006;2006(11):12–7. <https://doi.org/10.14227/DT130406P12>.
 24. Pleoger GF, Quizon PM, Abrahamsson B, Cristofolletti R, Groot DW, Parr A, Langguth P, Polli JE, Shah VP, Tajiri T, Mehta MU, Dressman J. Biowaiver Monographs for Immediate Release Solid Oral Dosage Forms: Cephalexin Monohydrate. *J Pharm Sci*. 2020;109:1846–62. <https://doi.org/10.1016/j.xphs.2020.03.025>.
 25. Prakash K, Raju NP, Kumari SK, Narasu LM. Solubility and Dissolution Rate Determination of Different Antiretroviral Drugs in Different pH Media Using UV Visible Spectrophotometer. *E-J Chem*. 2008;5(S2):1159–64. <https://doi.org/10.1155/2008/125917>.
 26. Nair A, Abrahamsson B, Barends DM, Groot DW, Kopp S, Polli EJ, Shah VP, Dressman JB. Biowaiver Monographs for Immediate-Release Solid Oral Dosage Forms: Primaquine Phosphate. *J Pharm Sci*. 2011;101:936–45. <https://doi.org/10.1002/jps.23006>.
 27. Verbeeck RK, Kanfer I, Löbenberg R, Abrahamsson B, Cristofolletti R, Groot DW, Langguth P, Polli JE, Parr A, Shah VP, Mehta M, Dressman JB. Biowaiver monographs for Immediate Release solid oral dosage forms: Enalapril. *J Pharm Sci*. 2017;106:P1933–1943. <https://doi.org/10.1016/j.xphs.2017.04.019>.
 28. Plöger GF, Abrahamsson B, Cristofolletti R, Groot DW, Langguth P, Mehta MU, Parr A, Polli JE, Shah VP, Tajiri T, Dressman JB. Biowaiver Monographs for Immediate Release Solid Oral Dosage Forms: Proguanil Hydrochloride. *J Pharm Sci*. 2018;107:1761–72. <https://doi.org/10.1016/j.xphs.2018.03.009>.
 29. Akdag Y, Gulsun T, Izat N, Oner L, Sahin S. Comparison of Dissolution Profiles and Apparent Permeabilities of Commercially Available Metformin Hydrochloride Tablets in Turkey. *Dissolution Technol*. 2020;2020(2):22–9. <https://doi.org/10.14227/DT270120P22>.
 30. Susantakumar P, Gaur A, Sharma P. Feasibility Biowaiver Extension of Immediate Release Oral Acyclovir 800 mg Tablet Formulations: A BCS Class III Drug. *Int J Pharm Pharmaceut Sci*. 2011;3:384–391. <https://innovareacademics.in/journal/ijpps/Vol3Issue4/2689.pdf>. Accessed 4 Jan 2024
 31. Jantratid E, Prakongpan S, Amidon GL, Dressman JB. Feasibility of Biowaiver Extension to Biopharmaceutics Classification System Class III Drug Products: Cimetidine. *Clin Pharmacokinet*. 2006;45:385–99. <https://doi.org/10.2165/00003088-200645040-00004>.
 32. Hassouna MEM, Issa YM, Zayed AG. A comparative study of the in-vitro dissolution profiles of paracetamol and caffeine combination in different formulations using HPLC. *J Applied Pharm Sci*. 2012;2:52–9. <https://doi.org/10.7324/JAPS.2012.2531>.
 33. Kassaye L, Genete G. Evaluation and comparison of in-vitro dissolution profiles for different brands of amoxicillin capsules. *Afr Health Sci*. 2013;13:369–75. <https://doi.org/10.4314/ahs.v13i2.25>.
 34. Thambavita D, Jayathilake CM, Sandamali KD, Galappaththy P, Jayakody RL. In Vitro Dissolution Testing to Assess Pharmaceutical Equivalence of Selected Amoxicillin Products Available in Sri Lanka: A Post-Marketing Study. *Dissolution Technol*. 2019;2019(2):56–61. <https://doi.org/10.14227/DT260119P56>.
 35. Strauch S, Jantratid T, Dressman JB, Junginger UE, Kopp S, Midha KK, Shah VP, Stavchansky S, Barends DM. Biowaiver Monographs for Immediate Release Solid Oral Dosage Forms: Lamivudine. *J Pharm Sci*. 2011;100:2054–63. <https://doi.org/10.1002/jps.22449>.
 36. FDA, Dissolution Testing and Acceptance Criteria for Immediate-Release Solid Oral Dosage Form Drug Products Containing High Solubility Drug Substances. Guidance for Industry, 2018. <https://www.fda.gov/media/92988/download>. Accessed 4 Jan 2024
 37. González-García I, Mangas-Sanjuan V, Merino-Sanjuán M, Álvarez-Álvarez C, Díaz-Garzón Marco J, Rodríguez-Bonnín MA, Langguth T, Torrado-Durán JJ, Langguth P, García-Arieta A, Bermejo M. IVIVC approach based on carbamazepine bioequivalence studies combination. *Pharmazie*. 2017;72:449–57. <https://doi.org/10.1691/ph.2017.7011>.
 38. Sjogren E, Westergren J, Grant I, Hanisch G, Lindfors L, Lennernas H, Abrahamsson B, Tannergren C. In silico predictions of gastrointestinal drug absorption in pharmaceutical product development: Application of the mechanistic absorption model GI-Sim. *Eur J Pharm Sci*. 2013;49:679–98. <https://doi.org/10.1016/j.ejps.2013.05.019>.
 39. Hartley R, Aleksandrowicz J, Bowmer CJ, Cawood A, Forsythe WI. Dissolution and relative bioavailability of two carbamazepine preparations for children with epilepsy. *J Pharm Pharmacol*. 1991;43:117–9. <https://doi.org/10.1111/j.2042-7158.1991.tb06644.x>.
 40. Pawar G, Wu F, Zhao L, Fang L, Burckart GJ, Feng K, Mousa YM, Al Shoyaib A, Jones M-C, Batchelor HK. Integration of Biorelevant Pediatric Dissolution Methodology into PBPK Modeling to Predict. *AAPS J*. 2023;25:67. <https://doi.org/10.1208/s12248-023-00826-1>.
 41. Macheras P, Argyrakos P. Gastrointestinal drug absorption: is it time to consider heterogeneity as well as homogeneity? *Pharm Res*. 1997;14(7):842–7. <https://doi.org/10.1023/a:1012183313218>.
 42. Charkoftaki G, Kytariolos J, Macheras P. Novel milk-based oral formulations: Proof of concept. *Int J Pharm*. 2010;390:150–9. <https://doi.org/10.1016/j.ijpharm.2010.001.038>.
 43. Trabelsi F, Gharavi N, Kalovidouris M, Nikolaidou M. Steady-state bioequivalence 2-way crossover study of two quetiapine prolonged-release 400 mg tablet formulations in normal male and female healthy subjects under fasting conditions. *Int J Clin*

- Pharmacol Ther. 2016;54(9):732–42. <https://doi.org/10.5414/CP202609>.
44. Macheras P, Koupparis M, Tsaprounis C. Drug dissolution studies in milk using the automated flow-injection serial dynamic dialysis technique. *Int J Pharm*. 1986;33:125–36. [https://doi.org/10.1016/0378-5173\(86\)90046-3](https://doi.org/10.1016/0378-5173(86)90046-3).
 45. Macheras P, Koupparis M, Apostolelli E. Dissolution of 4 controlled-release theophylline formulations in milk. *Int J Pharm*. 1987;36:73–9. [https://doi.org/10.1016/0378-5173\(87\)90239-0](https://doi.org/10.1016/0378-5173(87)90239-0).
 46. Jede C, Henze LJ, Meiners K, Bogdahn M, Wedel M, van Axel V. Development and Application of a Dissolution-Transfer-Partitioning System (DTPS) for Biopharmaceutical Drug Characterization. *Pharmaceutics*. 2023;15(4):1069. <https://doi.org/10.3390/pharmaceutics15041069>.
 47. Phillips DJ, Pygall SR, Cooper VB, Mann JC. Overcoming sink limitations in dissolution testing: a review of traditional methods and the potential utility of biphasic systems. *J Pharm Pharmacol*. 2012;64(11):1549–59. <https://doi.org/10.1111/j.2042-7158.2012.01523.x>.

Publisher's Note Springer Nature remains neutral with regard to jurisdictional claims in published maps and institutional affiliations.

Springer Nature or its licensor (e.g. a society or other partner) holds exclusive rights to this article under a publishing agreement with the author(s) or other rightsholder(s); author self-archiving of the accepted manuscript version of this article is solely governed by the terms of such publishing agreement and applicable law.